ChemComm

Accepted Manuscript

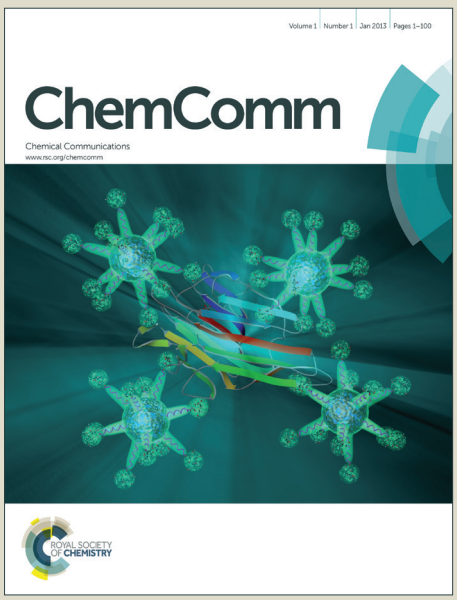

ROYAL SOCIETY OF CHEMISTRY

www.rsc.org/chemcomm

Journal Name

RSCPublishing

COMMUNICATION

Raising of the effective energy barrier promoted by the change of counteranion in a Zn-Dy-Zn SMM: Slow relaxation via the second excited state

Cite this: DOI: 10.1039/xoxxoooooox

Received ooth January 2012,
Accepted ooth January 2012

DOI: 10.1039/xoxxoooooox

www.rsc.org/

I. Oyarzabal,[a] J. Ruiz,[b] E. Ruiz,*[c] D. Aravena,[d] J. M. Seco*[a] and E. Colacio*[b]

The trinuclear complex [ZnCl(μ-L)Dy(μ-L)ClZn]PF_6 exhibits single-molecule magnet behaviour under zero field with a relatively large effective energy barrier of 186 cm^{-1}. *Ab initio* calculations reveal that the relaxation of the magnetization is symmetry-driven (the Dy^{III} ion possesses a C_2 symmetry) and occurs via the second excited state.

In recent years, much attention has been paid to zero-dimensional lanthanide coordination compounds exhibiting slow relaxation of the magnetization and magnetic hysteresis below a certain temperature known as blocking temperature (T_B).[1] These nanomagnets called single-molecule magnets (SMM's)[1] present potential future applications in fields such as molecular spintronics,[2] ultra-high density magnetic information storage[3] and as qubits for quantum computing at molecular level.[4] The SMM behaviour arises from the existence of an anisotropic energy barrier (U) that prevents magnetization reversal below T_B when the magnetic polarizing field is removed (the magnetization is frozen parallel the magnetic field).[1] The larger the energy barrier, the higher is T_B. Therefore, to increase the energy barrier and to improve the SMM properties, systems with large magnetic anisotropy must me designed.

[a] Departamento de Química Aplicada, Facultad de Química, Universidad del País Vasco UPV/EHU, Paseo Manuel de Lardizabal 3, 20018, Donostia-San Sebastian, Spain. Email: josemanuel.seco@ehu.es
[b] Departamento de Química Inorgánica, Facultad de Ciencias, Universidad de Granada, Av. Fuentenueva S/N, 18071 Granada, Spain. Email: ecolacio@ugr.es
[c] Departament de Química Inorgànica and Institut de Recerca de Química Teòrica i Computacional, Universitat de Barcelona, Diagonal 645, 08028, Barcelona, Spain. Email: eliseo.ruiz@qi.ub.es
[d] Departamento de Química de los Materiales, Facultad de Química y Biología,Universidad de Santiago de Chile (USACH), Casilla 40, Correo 33, Chile

† Electronic Supplementary Information (ESI) available: Synthesis of the ligand and complex, X-ray collecting data, shape measures, magnetic measurements details and ac plots, computational details and the spin density for the first 4 Kramers doublets. CCDC 1403753. See DOI: 10.1039/c000000x/

Lanthanide ions exhibit strong magnetic anisotropy due to the combination of strong spin-orbit coupling and crystal-field effects promoted by the ligand surrounding and therefore are excellent building blocks to be used in the construction of coordination compounds with SMM properties.[1] In fact, numerous 3d/4f and 4f (and 5f) mononuclear and polynuclear coordination compounds, most of them containing Dy^{III} ions,[1,5] have been shown to exhibit SMM behaviour. Interestingly, mononuclear and low-nuclearity 4f metal complexes have been shown to possess energy barriers an order of magnitude higher than observed in 3d and 3d/4f polymetallic clusters. The SMM behaviour observed for low-nuclearity 4f metal complexes generally is due to the individual Ln^{III} ions rather than to the whole molecule. Moreover, Ln···Ln interactions frequently favours fast quantum tunneling of the magnetization (QTM) in the ground state, which reduces the energy barrier to an effective value U_{eff}. Nevertheless, when the complex containing paramagnetic Ln^{III} ions is diluted in an isostructural diamagnetic lattice, the Ln···Ln interactions are reduced and the energy barrier often increases. It should be noted that although the U_{eff} values of Ln-based species are very large rarely show an open hysteresis loop at zero field, which is due to QTM. Theoretical and experimental studies carried out by us and others have shown that the incorporation of diamagnetic metal ions such as Zn^{II} in a Dy^{III} complex is a good strategy to enhance U_{eff}.[6] This fact could be due to two factors: (i) the quenching of the Ln···Ln interactions promoted by the presence of diamagnetic Zn^{II} ions (some kind of internal magnetic dilution) and (ii) the increase of electron density on the phenoxido oxygen donor atoms connecting the Zn^{II} and Dy^{III} ions provoked by the coordination to the Zn^{II} ions. By exploiting these features of the Zn^{II}/Dy^{III} systems and playing with the distribution of donor atoms on the Dy^{III} coordination environment following the guidelines of the simple prolate-oblate electrostatic model, we were able to rationally design a Zn-Dy-Zn SMM, [ZnCl(μ-L)Dy(μ-L)ClZn][$ZnCl_3(CH_3OH)$][6e] with a large effective energy barrier at zero-field.

In this paper we show how the replacement of the counteranion in the complex [ZnCl(μ-L)Dy(μ-L)ClZn][$ZnCl_3(CH_3OH)$][6e] (H_2L = N,N'-dimethyl-N,N'-bis(2-

hydroxy-3-formyl-5-bromo-benzyl)ethylenediamine; Figure 1) by PF_6^- affects the DyO_8 coordination environment leading to a important enhancement of the U_{eff}.

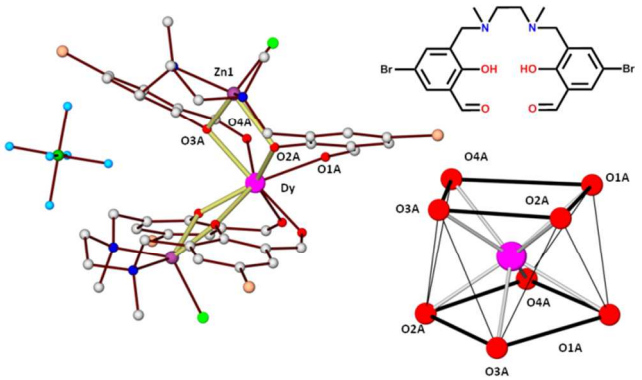

Fig. 1. Perspective view of complex **1**. The $Zn(O)_2Dy(O)_2Zn$ bridging fragment is given in bronze colour (left). Structure of the ligand (top right). Square-antiprism DyO_8 coordination sphere in **1** (bottom right).

The reaction of H_2L with $ZnCl_2$ and subsequently with $Dy(NO_3)_3{\cdot}5H_2O$ and KPF_6 in methanol affords well shaped yellow prismatic crystals of $[ZnCl(\mu\text{-}L)Dy(\mu\text{-}L)ClZn]PF_6$ (**1**). The X-ray crystal structure of **1** (Fig. 1; selected bond distances and angles are given as ESI) consists of $[ZnCl(\mu\text{-}L)Dy(\mu\text{-}L)ClZn]^+$ cations and PF_6^- anions. Within the trinuclear Zn–Dy–Zn cation, two $[ZnCl(L)]^-$ units are coordinated to the central Dy ion through the phenoxido and aldehyde oxygen atoms of the compartmental ligand L^{2-}, giving rise to a DyO_8 coordination polyhedron with Dy-$O_{phenoxide}$ distances of 2.340(3) Å and 2.275(3) Å and Dy-$O_{aldehyde}$ distances of 2.368(3) Å and 2.392(3) Å. The two halves of the trinuclear cation are symmetrically related by a C_2 axis passing through the Dy and P atoms.

Calculations of the degree of distortion of the DyO_8 coordination polyhedron with respect to an ideal eight-vertex polyhedron with continuous shape measure theory and the SHAPE software,[7] (see Table S3 in ESI) pointed out that the DyO_8 coordination polyhedron can be considered as intermediate between square antiprism, triangular dodecahedron and biaugmented triangular prism ideal polyhedra, but closer to the former geometry. In the square antiprism description, the average distance between the upper and lower planes containing the four oxygen atoms (two phenoxo and two aldehyde) is 2.565 Å, whereas the average distance of the sides of the squares defined by the oxygen atoms in each plane is 2.782 Å and therefore the distorted square-antiprism is compressed. Compared to $[ZnCl(\mu\text{-}L)Dy(\mu\text{-}L)ClZn][ZnCl_3(CH_3OH)]$, compound **1** shows a DyO_8 geometry that is closer to square antiprism (see Table S3) and presents a different distribution of the phenoxide oxygen atoms on the Dy^{III} coordination sphere (see below and Figure S5). Zn^{II} ions exhibit a distorted square-pyramid ZnO_2N_2Cl coordination environment, in which the nitrogen and phenoxide oxygen atoms occupy the basal positions with Zn-N bonds distances of 2.106 Å and 2.154 Å and Zn-O bond distances of 2.066 Å and 2.138 Å, whereas the axial position is occupied by the Cl atom at a longer distance of 2.217 Å. The Zn···Dy distance is 3.550(3) Å, whereas the Zn-Dy-Zn angle is 109.48(1)°. The shortest Dy···Dy distance between neighbouring $[ZnDyZn]^+$ trinuclear cations is 6.071(2) Å.

Direct-current (dc) magnetic susceptibility measurements were carried out on a randomly oriented polycrystalline sample of **1** in the 2-300 K temperature range and under an applied magnetic field of 0.1 T (Fig. 2, top left). The room temperature $\chi_M T$ value for **1** of 14.45 cm^3 K mol^{-1} is compatible with the calculated value of 14.17 cm^3 K mol^{-1} for the ground state of the Dy^{III} ion ($4f^9$, J =15/2, S = 5/2, L = 5, g = 4/3 $^6H_{15/2}$) in the free-ion approximation. On cooling, the $\chi_M T$ product decreases steadily to a value of 12.40 cm^3 K mol^{-1} at 5 K. Below this temperature, the $\chi_M T$ decreases sharply, reaching a value of 10.15 cm^3 K mol^{-1} at 2 K. This behaviour is associated with the magnetic anisotropy of the Dy^{III} ion and possible weak intermolecular interactions, which could be responsible for the sharp decrease in $\chi_M T$ below 5 K. The field dependence of the magnetization at 2 K shows a relatively rapid increase at low field reaching almost saturation for magnetic fields larger than 2 T. The saturation value of 5.10 $N\mu_B$ agrees well with those observed for Dy^{III} complexes with strong magnetic anisotropy.[6]

In order to know if **1** exhibits SMM properties, dynamic alternating-current (ac) magnetic measurements were performed as a function of both temperature and frequency on a microcrystalline powder sample (Fig. 2, top right and Fig. S1-S3 in ESI). At zero *dc* field, **1** exhibits a strong frequency dependence of the out-of-phase susceptibility (χ_M") signals below 35 K, which clearly indicates the occurrence of slow relaxation of the magnetization and SMM behaviour in this compound. This behaviour is not surprising in view of the easy-axis anisotropy of the Dy^{III} ion (see below for *ab initio* calculations). The fact that both χ'_M and χ''_M components do not go to zero below the maxima at low temperature, points out to the existence of fast relaxation of the magnetization via a QTM mechanism. The Cole-Cole plot (Fig. S2 in ESI) shows semicircular shapes with α values in the 0.28 (17 K)-0.04 (25 K) range, thus suggesting the existence of multiple relaxation processes.

The relaxation times extracted from the frequency-dependent susceptibility data in the 18-27 K range were fitted to the Arrhenius law, affording an effective energy barrier for the reversal of the magnetization of 186 cm^{-1} with $\tau_0 = 4.98{\cdot}10^{-10}$ s (Fig. 2, bottom left).

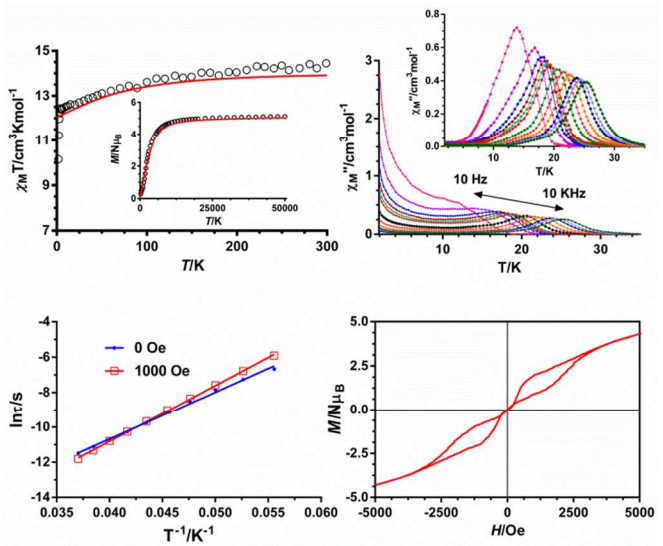

Fig. 2. Temperature dependence of $\chi_M T$ for **1** (top, left). Temperature dependence of the out-of-phase χ"$_M$ component of the ac magnetic susceptibility for **1** under zero and 1000 Oe (inset) applied magnetic fields at different frequencies (top, right). Arrhenius plots for the relaxation times (τ) extracted from the χ_M" *vs f* data in zero and 1000 Oe

dc fields for **1** (bottom, left). Magnetic hysteresis loops for **1** within -5 < *H*/kOe < 5 at 2K.

When the ac measurements on **1** were performed in the presence of a small external dc field of 1000 Oe (this field was chosen because under its application the relaxation process was shown to be the slowest) to partly or fully suppress the QTM, the tails at low temperatures almost disappeared and the high temperature peaks remained at similar temperatures and with comparable intensities to those observed under zero dc applied field (Fig. 3, inset). The fit of the relaxation times in the 18-27 K to the Arrhenius law leads, as expected, to an increase of the thermal energy barrier and a decrease of τ_0 (U_{eff} = 222 cm^{-1} with $\tau_0 = 5.66 \cdot 10^{-11}$ s). In the high temperature region, the α values extracted from the Cole-Cole plot (Fig. S2 in the ESI) are in the 0.22 (19 K)-0.08 (25 K) range, which points to the existence of a distribution of the relaxation times.

The energy barrier for **1** is approximately twice that of $[ZnCl(\mu\text{-}L)Dy(\mu\text{-}L)ClZn][ZnCl_3(CH_3OH)]$.[6e] With the aim of rationalizing this surprising increase of the energy barrier promoted by the change of counteranion, we have performed *ab initio* electronic calculations based on the CASSCF+RASSI/SINGLE_ANISO[8] method using MOLCAS 7.8 code[9] (Table S5). The energy spectrum of the eight Kramers doublets (KDs) spans up to 491.8 cm^{-1} and the energy gap between the ground and first excited is 144 cm^{-1}, which are rather normal values for Dy^{III} complexes. The ground Kramers doublet (KD1) is almost pure $m_J = \pm 15/2$ with effective g_z and $g_{x,y}$ values approaching to 20 and zero, respectively. Therefore KD1 is an almost ideal Ising state which favours the slow relaxation of the magnetization and the SMM behaviour, in accordance with the zero-field SMM properties observed for **1**. It is worth mentioning that the *ab initio* calculations accurately reproduce the direct current (dc) magnetic susceptibility and magnetization data for **1** (Fig. 2 top left), which gives confidence in the calculated low-lying KDs energies. The main magnetic axis of the KD1 lies close to the two Dy-O2A vectors (Fig. 3), which shows the tendency of this axis to point to the donor atoms with greater electron density and shorter Dy-O distances (O2A phenoxide bridging atoms of the ligands with Dy-O2A = 2.275 Å). This orientation of the magnetic moment forces the oblate electron density of the Dy^{III} to be perpendicular to the O2A atoms thus diminishing electrostatic repulsions. The O2A phenoxido atoms are roughly located at axial positions on the DyO_8 coordination sphere, thus emphasizing the suitability of an axially repulsive coordination environment for achieving SMM properties in Dy^{III} compounds, as qualitatively anticipates the oblate-prolate model.[1b] DFT calculations of the electrostatic potential maps provoked by the ligands projected on the Dy^{III} position (Fig. 3 right) agree with the above qualitative electrostatic predictions.

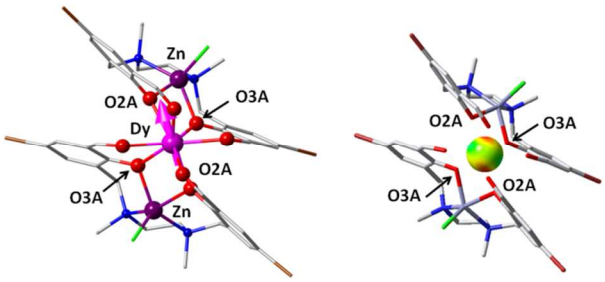

Fig. 3. (Left) *Ab initio* computed orientation of the magnetic moment of the ground state for **1** (pink arrow). (Right) DFT calculated (B3LYP/TZV) electrostatic potential of the coordination environment (only ligands) projected in a sphere located at the Dy position (1 Å radius). Yellow-green regions on the sphere correspond to low potential (less repulsive) while highly repulsive regions are indicated as red spots.

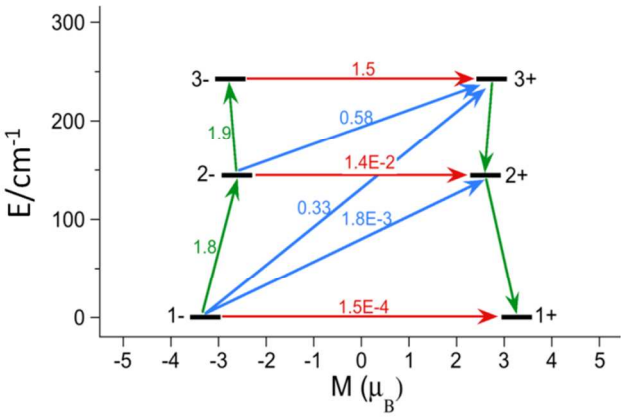

Fig. 4. Lowest three Kramers doublets (KDs) and *ab initio* computed relaxation mechanism in **1.** The thick black lines imply KDs as a function of their magnetic moment along the main anisotropy axis.The red lines correspond to ground state QTM and TA-QM via the first and second excited KDs, blue lines show possible Orbach relaxation processes. The values indicated close to the arrows indicate the matrix elements of the transition magnetic moments.

Thus, the oblate beta electron density of the ground state (which is formed by mixing in the ground RASSI wave function the two first, almost degenerate, states in the CASSCF step; Fig. S4 and Table S6) is hosted in the region with less repulsion (yellow-green in Fig. 3, right) whereas the magnetic moment is pointing towards the strongest repulsion regions (red in Fig. 3, right)

It should be noted that the extracted effective energy barrier at zero *dc* field is 40 cm^{-1} larger than the energy gap between the ground and first excited KDs and therefore the relaxation of the magnetization cannot take place via the first excited state. However, the relaxation could occur through the second excited KD, which would be located 243.3 cm^{-1} above the ground KD. In such a case, the extracted U_{eff} would be lower than predicted by electronic structure calculations, which could be justified by the existence of fast QTM relaxation. In fact, the value of energy barrier extracted from the *ac* measurements under an applied *dc* field of 1KOe (U_{eff} = 222 cm^{-1}), when the QTM relaxation is almost suppressed, is close to the energy of the second excited state. The relaxation via the first excited state is suppressed because the main anisotropy axes of the ground and first excited states (the latter is an almost pure Ising state with $m_j = \pm 13/2$, g_z ~17 and $g_{x,y}$ <0.05) are not only Ising like, but also almost parallel (the angle is 2.4°). The collinearity of the principal anisotropy axes up to the first excited KD, which is due to the presence of a C_2 axis around the Dy^{III} ion, blocks Orbach relaxation.[6d,10]

In order to probe the magnetization relaxation mechanism in **1**, we have computed the transition magnetic moment matrix elements between the connecting pairs of opposite magnetization (Fig. 4 and Figure S6). Owing to the almost pure Ising nature of the ground state, QTM is expected to be very weak, which is supported by the low magnitude of the transition magnetic moment element between the ground state KDs (~10^{-4} μ_B). This must be the reason why **1** exhibits SMM behaviour at zero field. The same argument can be used to justify the absence of thermally-assisted quantum tunnelling of magnetization (TA-QTM) through the first excited state. However, the TA-QTM mechanism via the second excited KD (± 3 states) becomes

dominant as it exhibits the largest value of the transition magnetic moment element (1.5 μ_B). As expected for the collinearity of the main anisotropy axes of the ground and first excited KDs, the off diagonal term connecting these KD (related with the Orbach process) is very small (~10^{-3} μ_B). Nevertheless, the Orbach process is operative via the second excited state as the transversal magnetic moments are moderate (0.33 and 0.58 μ_B). Therefore, the relaxation of the magnetization occurs through the second excited state via Orbach/TA-QTM processes.

Although the Dy-O distances in **1** and [ZnCl(μ-L)Dy(μ-L)ClZn][$ZnCl_3(CH_3OH)$][6e] are very similar, the fact that the former exhibits a C_2 symmetry axis around the Dy^{III} ion forces the phenoxido oxygen atoms to adopt a different distribution in the Dy^{III} coordination sphere with respect to that observed for the latter (in **1** the phenoxide oxygen atoms are closer to each other and the Zn-Dy Zn angle is much smaller, 109.48° vs 141.7°; see Fig. 1 left and Figure S5), which would ultimately be responsible for the relaxation mechanism through the second excited KD.

At 2 K and using the sweep rate accessible in a conventional SQUID magnetometer, compound **1** exhibits a butterfly shaped hysteresis loop with almost negligible magnetization at zero field (Fig. 2 bottom, right), which is consistent with the QTM generally found for 4f containing complexes and with the tail that **1** exhibits at low temperature in the χ_M" *vs T* plot at zero applied field.

In summary, we have shown how the replacement of the counteranion in a Zn-Dy-Zn trinuclear complex provokes a change towards a more symmetric structure where there exists a C_2 axis on the Dy^{III} ion. The presence of the C_2 axis imposes collinearity of the anisotropic axes of the two lowest KDs, so that the thermal activated relaxation is suppressed via the first excited KD and takes place via the second excited state, giving rise to a dramatic increase in the effective energy barrier. This is one of the few cases where this type of symmetry-driven relaxation mechanism has been observed [6d,10b,c] and the first case where it is due to a structural change promoted by the replacement of the counteranion.

Financial support from UPV/EHU for project GIU14/01 and Ministerio de Economía y Competitividad (MINECO) for Projects CTQ-2011-24478, CTQ2011-23862-C02-01 and CTQ2014-56312-P, the University of Granada and Junta de Andalucía (FQM-195 and the Project of excellence P11-FQM-7756) are grateful acknowledged. E.R. thanks Generalitat de Catalunya for an ICREA Academia fellowship. D.A. thanks CONICYT+PAI "Concurso nacional de apoyo al retorno de investigadores/as desde el extranjero, convocatoria 2014 82140014" for financial support. I. O. is grateful to the Departamento de Educación, Universidades e Investigación del Gobierno Vasco for a predoctoral fellowship. Technical and human support provided by SGIker (UPV/EHU, MINECO, GV/EJ, ERDF and ESF) is gratefully acknowledged.

Notes and references

1 (a) R. A. Layfield and M. Murugesu (eds), *Lanthanides and Actinides in Molecular Magnetism*, Wiley-VCH, Weinheim, Germany, 2015; (b) J. D. Rinehart and J. R. Long, *Chem. Sci.,* 2011, **2**, 2078; (c) Y. N. Guo, G. F. Xu, Y. Guo and J. Tang, *Dalton Trans.,* 2011, **40**, 9953; (d) L. Sorace, C. Benelli and D. Gatteschi, *Chem. Soc. Rev.*, 2011, **40**, 3092; (e) J. Luzon and R. Sessoli, *Dalton Trans*., 2012, **41**, 13556; (f) J. M. Clemente-Juan, E. Coronado and A. Gaita-Ariño, *Chem. Soc. Rev.,* 2012, **41**, 7464; (g) D. N. Woodruff, R. E. P Winpenny and R. A. Layfield, *Chem. Rev*., 2013, **113**, 5110; (h) P. Zhang, Y.-N. Guo and J. Tang, *Coord. Chem. Rev.,* 2013, **257**, 1728.

2 (a) L. Bogani and W. Wernsdorfer, *Nat. Mat.,* 2008, **7**, 179;; (b) R. Vincent, S. Klyatskaya, M. Ruben, W. Wernsdorfer and F. Balestro, *Nature,* 2012, **488**, 357; (c) M. Ganzhorn, S. Klyatskaya, M. Ruben and W. Wernsdorfer, *Nature Nanotech*., 2013, **8**, 165; (d) M. Jenkins, T. Hümmer, M. J. Marínez-Pérez, J. García-Ripoll, D. Zueco and F. Luis, *New. J. Physics*, 2013, **15**, 095007.

3 (a) A. R. Rocha, V. M. García-Suárez, S. W. Bailey, C. J. Lambert, J. Ferrerand and S. Sanvito, *Nat. Mater.,* 2005, **4**, 335; (b) M. Affronte, *J. Mater. Chem*., 2009, **19**, 1731.

4 (a) M. N. Leuenberger and D. Loss, *Nature*, 2001, **410**, 789; (b) A. Ardavan, O. Rival, J. J. L. Morton, S. J. Blundell, A. M. Tyryshkin, G. A. Timco and R. E. P. Winpenny, *Phys. Rev. Lett.*, 2007, **98**, 057201; (c) P. C. E. Stamp and A. Gaita-Ariño, *J. Mater. Chem*., 2009, **19**, 1718; (d) M. J. Martínez-Pérez, S. Cardona-Serra, C. Schlegel, F. Moro, P. J. Alonso, H. Prima-García, J. M. Clemente-Juan, M. Evangelisti, A. Gaita-Ariño, J. Sesé, J. Van Slageren, E. Coronado and F. Luis, *Phys. Rev. Lett*., 2012, **108**, 247213.

5 (a) R. Sessoli and A. K. Powell, *Coord. Chem. Rev.*, 2009, **253**, 2328; (b) M. Andruh, J. P. Costes, C. Diaz and S. Gao, *Inorg.Chem*., 2009, **48**, 3342 (Forum Article); (c) "Molecular Magnets", themed issue (Brechin, E. K. Ed.), *Dalton Trans*., 2010.

6 (a) A. Watanabe, A. Yamashita, M. Nakano, T. Yamamura and T. Kajiwara, *Chem. Eur. J*., 2011, **17**, 7428; (b) J.-L. Liu, Y.-C. Chen, Y.-Z. Zheng, W.-Q. Lin, L. Ungur, W. Wernsdorfer, L. F. Chibotaru and M.-L. Tong, *Chem. Sci*., 2013, **4**, 3310; c) S. Titos-Padilla, J. Ruiz, J. M. Herrera, E. K. Brechin, W. Wersndorfer, F. Lloret, E. Colacio, *Inorg. Chem*., 2013, **52**, 9620; d) A. Upadhyay, S. Kumar Singh, C. Das, R. Mondol, S. K. Langley, K. S. Murray, G. Rajaraman and M. Shanmugam, *Chem. Commun*., 2014, **50**, 8838; (e) I. Oyarzabal, J. Ruiz, J. M. Seco, M. Evangelisti, A. Camón, E. Ruiz, D. Aravena and E. Colacio, *Chem. Eur. J*., 2014, **20**, 14262; (j) K. S. Bejoymohandas, A. Dey, S. Biswas, M. L. P. Reddy, R. Morales, E. Ruiz, S. Titos-Padilla, E. Colacio and V. Chandrasekhar, *Chem. Eur. J*., 2015, **21**, 6449.

7 M. Llunell, D. Casanova, J. Cirera, J. M. Bofill, P. Alemany, S. Alvarez, M. Pinsky and D. Avnir, SHAPE v1.1b, Barcelona, 2005.

8 (a) P. A. Malmqvist, B. O. Roos and B. Schimmelpfennig, *Chem. Phys. Lett.,* 2002, **357**, 230; (b) L. F. Chibotaru and L. J. Ungur, *Chem. Phys.* 2012, **137**, 064112.

9 (a) J. A. Duncan, *J. Am. Chem. Soc.,* 2009, **131**, 2416; (b) F. Aquilante, L. De Vico, N. Ferre, G. Ghigo, P. A. Malmqvist, P. Neogrady, T. B. Pedersen, M. Pitonak, M. Reiher, B. O. Roos, L. Serrano-Andres, M. Urban, V. Veryazov and R. Lindh, *J. Comput. Chem*., 2010, **31**, 224; (c) V. Veryazov, P. O. Widmark, L. Serrano-Andres, R. Lindh and B. O. Roos, *Int. J. Quantum Chem.* 2004, **100**, 626; (d) G. Karlstrom, R. Lindh, P. A. Malmqvist, B. O. Roos, U. Ryde, V. Veryazov, P. O. Widmark, M. Cossi, B. Schimmelpfennig, P. Neogrady, L. Seijo, *Comput. Mater. Sci.,* 2003, **28**, 222.

10 (a) R. J. Blagg, L. Ungur, F. Tuna, J. Speak, P. Comar, D. Collison, W. Wernsdorfer, E. J. L. McInnes, L. F. Chibotaru and R. E. P. Winpenny, 2013, **5**, 2013; (b) Y.-N. Guo, L. Ungur, G. E. Granroth, A. K. Powell, C. Wu, S. E. Nagler, J. Tang, L. F. Chibotaru and D. Cui, *Sci. Rep*., 2014, **4**, 5471; (c) S. K. Singh, T. Gupta, M. Shanmugam and G. Rajaraman, *Chem. Commum.,* 2014, **50**, 15513.

